Spectral-Spatial Pulse Design with Spectral Decomposition

C. Yang[1], and V. A. Stenger[1]
[1]University of Hawaii, Honolulu, Hawaii, United States

Introduction: Signal loss caused by susceptibility induced intravoxel dephasing is a major limitation in high field MRI applications such as BOLD fMRI. Spectral-spatial (SPSP) pulses have been shown to be very effective at reducing through-plane signal loss in axial slices using a single excitation [1,2]. SPSP pulse design assumes a linear relationship between off-resonance frequency and through-plane susceptibility gradient $G_s(f)=\alpha f$. Previous studies show empirically α=-2.0 μT/m/Hz works well for many brain regions at 3T, however, no detailed measurement of α was investigated. We propose spectral decomposition technique [3] using a spiral spectroscopic imaging sequence to directly measure α at all locations in the brain. Resultant SPSP pulses were demonstrated in T2*-weighted brain images showing reduced signal loss at 3T. Inferior slices were found to require α values of opposite sign and smaller magnitude. This indicates that using more than one pulse may improve the efficacy of the SPSP technique.

Theory: The induced signal loss in a slice at TE can be compensated by time-shifting the RF pulse by $\Delta\tau(f) = G_s(f)\mathrm{TE}/G_z$ relative to the slice-select gradient G_z [3-4]. The signal s in a pixel in a region with signal loss can be shown to be:

$$s = \Delta z m_0 \mathrm{sinc}\left[\gamma \Delta z (G_z \Delta\tau - G_s(f)\mathrm{TE})/2\right].$$

Here m_0 is magnetization and Δz slice thickness. A pixel in a slice can be can spectrally decomposed to determine $G_s(f)$ by incrementally adjusting the shift of the RF pulse each TR in a spectroscopic imaging sequence. Figure (a) shows a spiral spectroscopic imaging sequence with shifted RF pulse. Figure (b) shows an example of a spectrally decomposed slice displayed as a function of shift and frequency. Note the sinc profile along the shift direction as well as the presence of "lost" signal located off resonance as highlighted by the circle. Fits to the peak pixel value can be used to determine α, which can then be used in the SPSP pulse design.

Methods: Human brain scans were performed on a Siemens 3T Trio scanner with 180T/m/s slew rate and 4mT/m peak gradient. A spiral spectroscopic imaging sequence with 30 readouts and 30 pulse shifts (50μs increments, G_z=2.8 mT/m) was used for spectral decomposition (12 64x64 5mm axial slices, 4 interleaves, 22cm FOV, 2000ms TR, 30ms TE, 4:00 scan time). Fits for α were then determined for all spatial locations. SPSP RF and gradient pulse profiles were calculated using Matlab [1]. The SPSP pulses were utilized in a FLASH sequence (12 128x128 5mm axial slices, 22cm FOV, TR/TE=1000/30ms, 2:08 scan time) on healthy volunteers.

Results: Figure (c) shows an example of two slices in one human subject. Two areas with signal loss A1 and A2 were observed in slices 1 and 2 and fits for α1 and α2 were determined. The α2 for the superior slice was in good agreement with -2.0μT/m/Hz. The α1 for the inferior slice, however, required 1.0μT/m/Hz, which is opposite in sign and smaller magnitude. A SPSP pulse was designed for α1 and α2 and the slices were re-acquired. Figure (e) shows the slices acquired with a standard pulse and the pulses for α1 and α2. The inferior slice shows better signal recovery with α1 and the superior slice with α2.

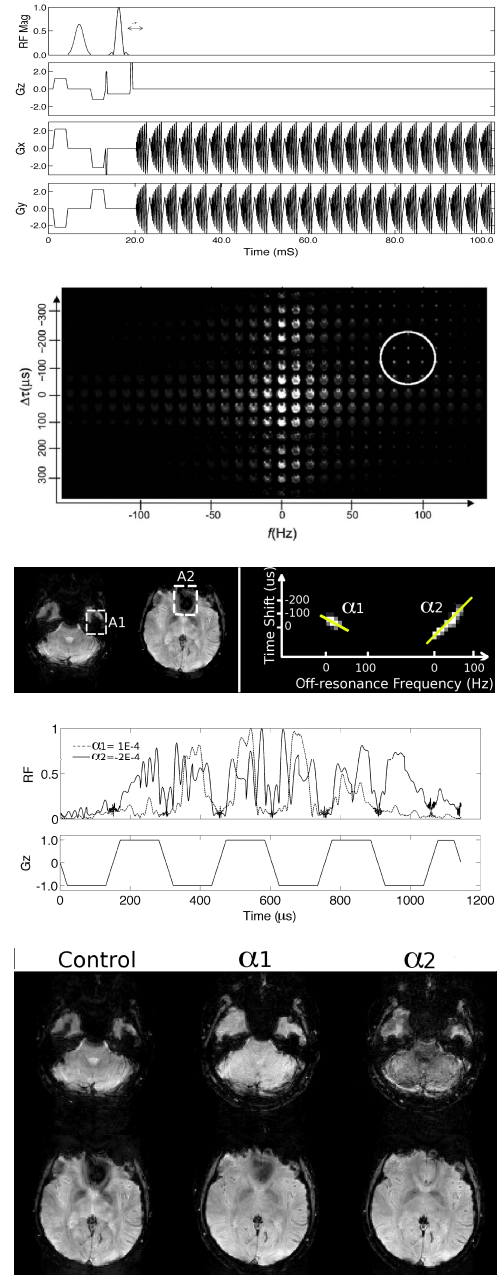

Discussion: Spectral decomposition revealed that more than one SPSP pulse can improve loss recovery in T2*-weighted applications such as BOLD fMRI. It may be possible to use spectral decomposition as a pre-scan routine to determine a SPSP pulse for each slice in a subject. Future work will be to implement the pulses in an fMRI sequence to examine BOLD signal recovery.

References: (1) C-Y Yip *et al*. MRM 2009:V61:I5:1137:1147. (2) C. Yang *et al.* MRM 2010 V64:I1:1:8. (3) Y.M. Ro et al. MRM 1995 V33:I4:521:528. (4) W. Deng *et al.* MRM 2009 V61:I2:255:258.

Acknowledgments: Work supported by the NIH (R01DA019912, R01EB011517, K02DA020569). Core resources supported by the NCRR (G12-RR003061, P20-RR011091), NINDS (U54-NS56883), and the ONDCP.